Clin Orthop Relat Res (2012) 470:329–338
DOI 10.1007/s11999-011-2057-x

Clinical Orthopaedics and Related Research®
A Publication of The Association of Bone and Joint Surgeons®

SYMPOSIUM: PAPERS PRESENTED AT THE ANNUAL MEETINGS OF THE HIP SOCIETY

# The John Charnley Award

## An Accurate and Sensitive Method to Separate, Display, and Characterize Wear Debris

## Part 1: Polyethylene Particles

**Fabrizio Billi PhD, Paul Benya PhD, Aaron Kavanaugh BS, John Adams MD, PhD, Edward Ebramzadeh PhD, Harry McKellop PhD**

Published online: 14 October 2011


**Abstract**

*Background* Numerous studies indicate highly crosslinked polyethylenes reduce the wear debris volume generated by hip arthroplasty acetabular liners. This, in turns, requires new methods to isolate and characterize them.

*Questions/purposes* We describe a method for extracting polyethylene wear particles from bovine serum typically used in wear tests and for characterizing their size, distribution, and morphology.

*Methods* Serum proteins were completely digested using an optimized enzymatic digestion method that prevented the loss of the smallest particles and minimized their clumping. Density-gradient ultracentrifugation was designed to remove contaminants and recover the particles without filtration, depositing them directly onto a silicon wafer. This provided uniform distribution of the particles and high contrast against the background, facilitating accurate, automated, morphometric image analysis. The accuracy and precision of the new protocol were assessed by recovering and characterizing particles from wear tests of three types of polyethylene acetabular cups (no crosslinking and 5 Mrads and 7.5 Mrads of gamma irradiation crosslinking).

*Results* The new method demonstrated important differences in the particle size distributions and morphologic parameters among the three types of polyethylene that could not be detected using prior isolation methods.

*Conclusion* The new protocol overcomes a number of limitations, such as loss of nanometer-sized particles and artifactual clumping, among others.

*Clinical Relevance* The analysis of polyethylene wear particles produced in joint simulator wear tests of prosthetic joints is a key tool to identify the wear mechanisms that produce the particles and predict and evaluate their effects on periprosthetic tissues.

One or more of the authors has received funding from NIH/NIAMS (FB, PB, JA), Medtronic Sofamor Danek, Inc (Minneapolis, MN, USA) (FB, EE), Wright Medical Technology, Inc (Arlington, TN, USA) (FB), DePuy Orthopaedics, Inc (Warsaw, IN, USA) (FB, HM), Stryker Orthopaedics (Mahwah, NJ, USA) (FB), and Biomet, Inc (Warsaw, IN, USA) (FB). One or more of the authors (HM) has received royalties from DePuy.
Each author certifies that his or her institution approved or waived approval for the reporting of this investigation and that all investigations were conducted in conformity with ethical principles of research.
This is a companion article to Billi F, Benya P, Kavanaugh A, Adams J, PhD, McKellop H, Ebramzadeh E. The John Charnley Award. An Accurate and Extremely Sensitive Method to Separate, Display, and Characterize Wear Debris. Part 2: Metal and Ceramic Particles. *Clin Orthop Relat Res.* 2011. DOI 10.1007/s11999-011-2058-9

**Electronic supplementary material** The online version of this article (doi:10.1007/s11999-011-2057-x) contains supplementary material, which is available to authorized users.

F. Billi (✉), P. Benya, A. Kavanaugh, J. Adams, E. Ebramzadeh, H. McKellop
The J. Vernon Luck Sr., MD, Orthopaedic Research Center at Orthopaedic Hospital, UCLA/Orthopaedic Hospital, Department of Orthopaedic Surgery, David Geffen School of Medicine, Los Angeles, CA 90007, USA
e-mail: fbilli@laoh.ucla.edu

## Introduction

Wear particles are recognized as one of the major causes of osteolysis leading to failure in total joint arthroplasties. With the introduction of highly wear-resistant crosslinked ultrahigh-molecular-weight polyethylene (UHMWPE), the overall volume of wear debris in THA has decreased compared to conventional polyethylene (PE) from more

than 15 $mm^3$/million cycles to less than 1 $mm^3$/million cycles, particularly in THAs [9, 37]. The reduction in overall PE wear rates has resulted in an associated and substantial reduction in the rates of osteolysis, with several clinical studies reporting no incidence at 5 to nearly 10 years' followup [10, 13, 19, 20, 27, 32, 39]. Furthermore, wear particles of specific shapes, such as fibrils or needles, that elicit higher cellular reaction [14, 15, 49] have been minimized.

The average size of crosslinked PE is reported to be smaller than conventional PE [40, 47]. Combined with the reduced volume, this poses new challenges in purification, isolation, and characterization of nanometer-sized particles because even a small loss of particles through the digestion process or overestimation of size due to artifactual clumping can greatly skew the size distribution and morphologic analysis.

This may explain why models developed for conventional UHMWPE to evaluate the biologic response to particles have predicted higher osteolytic potential for crosslinked PEs [16, 26] rather than the lower potential actually observed. To date, methods developed to assess the biologic reactivity to wear debris have considered the sizes, compositions, and surface areas of the particles [22, 30, 33, 44, 45]. However, a careful reevaluation of the biologic activity for crosslinked PE should take into account the overall volume in addition to the particle size, composition, and area and should be based on a highly precise method for obtaining purified and well-characterized PE particles.

Images obtained with previous protocols showed clumping of particles and extensive residue and contaminants, suggesting incomplete digestion and inadequate separation of particles. As a result, image analysis and characterization of the particles were difficult if not impossible. Additionally, the amount of wear found in joint simulator wear tests of crosslinked PE did not correspond to the number of particles observed, suggesting possible particle loss during the isolation process.

Our research center has been previously instrumental in the development of techniques to isolate and characterize PE particles from metal-on-polyethylene THAs [6, 7, 35, 43]. Expanding on this earlier experience, we have now developed a novel protocol to meet the demands of analyzing newer crosslinked PE particles including enhanced particle separation, purification, and particle display. This protocol produces minimal artifactual clumping; better image contrast; and more sensitive, more reproducible, and more accurate size distribution and morphometric analysis of highly purified authentic wear particles. We describe our approach and our efforts to validate our protocol with control particles having the same size and shape distribution as the in vitro samples.

## Materials and Methods

An overview of the experimental procedure is outlined (Fig. 1). Wear particles were extracted from serum lubricant using an optimized enzymatic digestion protocol. This was followed by an innovative display on a silicon wafer and subsequent morphometric analysis, coupled with a novel algorithm to automatically classify the particles by shape and size.

To evaluate the utility and sensitivity of the optimized protocol, we isolated and characterized the particles generated in hip simulator tests of three types of PE (Table 1), ie, noncrosslinked and 5-Mrad and 7.5-Mrad crosslinked. These PEs were included because the effect of crosslinking on the size and morphology of the particles was examined in several prior studies with varying results [1, 4, 12, 41, 42]. Two types of crosslinked PE were included to demonstrate the ability of the protocol to detect subtle differences between the two materials.

We performed wear testing using a hip simulator (Shore Western Manufacturing Inc, Monrovia, CA, USA) under a double-peaked load profile (maximum, 2000 N) [34]. The lubricant was 90% filtered bovine serum (HyClone, Logan, UT) treated with ethylenediaminetetraacetic acid (EDTA) and sodium azide ($NaN_3$) to a final concentration of 20 mmol/L and 0.2% w/v, respectively. EDTA was added to minimize precipitation of calcium phosphate onto the bearing surface [29] and $NaN_3$ was used to eliminate bacterial contamination and lubricant degradation.

Three samples of serum lubricant were obtained after 1.25 million wear cycles from each of three simulator test stations for the three types of PE. We processed samples from each test station and PE type using two digestion-isolation protocols (Fig. 1). Each sample was analyzed in triplicate for a total of 54 samples. Before processing, we rotated the nine lubricant samples end-over-end at 28 rpm for 48 hours at room temperature to evenly suspend the particles in the lubricant.

The first protocol, originally developed at our research center in the 1990s [8], has been widely used [24, 31, 46, 48] and is hereinafter referred to as the NaOH protocol. Briefly, samples were digested with 5 N NaOH, layered above a sucrose density gradient, and submitted to ultracentrifugation, and the floating particles were collected on a polycarbonate (PC) filter membrane (0.01 μm) for analysis via a field emission scanning electron microscope (FE-SEM) (Supra VP-40; Zeiss, Peabody, MA, USA). The second protocol, introduced in this study, is hereinafter referred to as the silicon wafer display (SWD) protocol, since the particles are collected on a 5- × 5-mm featureless display silicon wafer (Ted Pella, Inc, Redding, CA, USA), without filtration. The protocol consisted of a

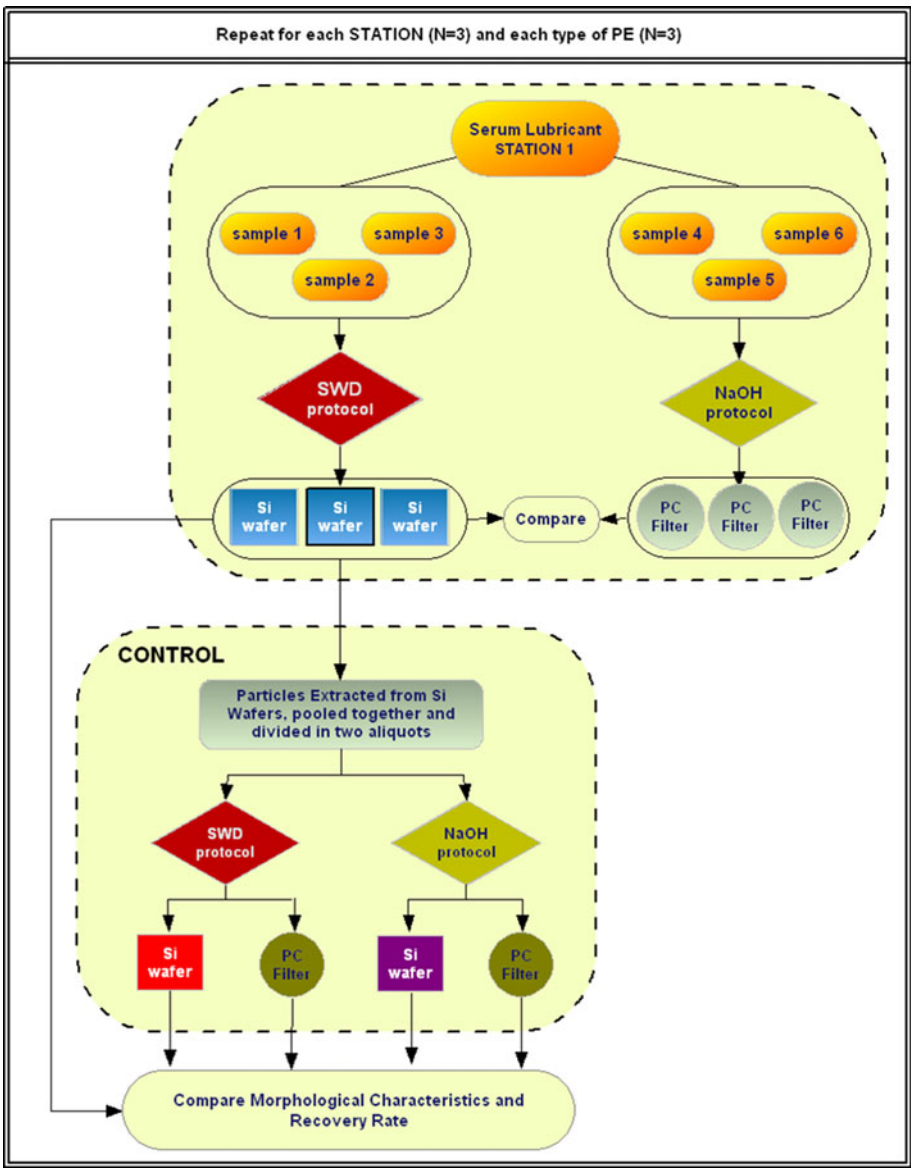


**Fig. 1** A flowchart shows an outline of the experiment.

series of optimized steps (Fig. 2) (Appendix 1; supplemental materials are available with the online version of CORR).

Digestion of lubricant proteins with proteinase K in the presence of urea and calcium was chosen because denaturation of proteins due to urea-dependent cleavage of hydrogen bonds leads to more complete proteolytic digestion [23] without the complications of detergents. Inclusion of calcium during digestion partially protected the proteinase K from autodigestion in urea [2]. After digestion, calcium was chelated with excess EDTA to reverse any divalent cation-dependent peptide linkages, and disulfide bonds were broken with tris(2-carboxyethyl)phosphine; both steps led to the smallest possible peptide digestion products.

We obtained purification of the particles in a three-step ultracentrifugation process (Fig. 2, purification). The rationale behind each step is reported in Appendix 1. Briefly, in Step 1, particles were concentrated into a detergent (sodium lauroyl sarcosine [SLS])/urea layer to solubilize lipid and disperse particles without aggregation. In Step 2, the particles entered a continuous isopropyl alcohol (IPA) gradient that stripped SLS from them. Step 3 concentrated the particles at the sharp 10%:50% IPA interface and further separated the particles from residual detergent.

For counting and morphometric analysis, PE particles were diluted in water and floated onto an inverted, silicon wafer coated with marine mussel glue (Cell-Tak™; BD Biosciences, San Jose, CA, USA) (details in Appendix 1) by centrifugation (Fig. 2, isolation). This technique was

intended to minimize aggregation of PE particles, which moved parallel to the centrifugal force and to the tube walls, thus evenly depositing them on the surface of the wafer (Fig. 3).

**Table 1.** Types of polyethylene used to generate wear debris

| Type of polyethylene | Processing |
|---|---|
| Noncrosslinked | GUR 1050 extruded rod |
| | Machined into cups |
| | Sterilized with gas plasma |
| Crosslinked at 5 Mrads | GUR 1050 extruded rod |
| | Crosslinked with 5 Mrads gamma radiation |
| | Remelted at 155°C for 24 hours to extinguish residual free radicals, annealed at 120°C for 24 hours (both processes under partial vacuum), and then slowly cooled to room temperature |
| | Machined into cups |
| | Sterilized with gas plasma |
| Crosslinked at 7.5 Mrads | GUR 1020 extruded rod |
| | Crosslinked with 7.5 Mrads gamma radiation |
| | Remelted at 155°C for 24 hours to extinguish residual free radicals, annealed at 120°C for 24 hours (both processes under partial vacuum), and then slowly cooled to room temperature |
| | Machined into cups |
| | Sterilized with gas plasma |

To characterize the particles, the wafer was glued to an aluminum stub, coated with 10 Å iridium (EBS; SouthBay Technology, San Clemente, CA, USA), and imaged in a FE-SEM at a voltage of 13 kV. We imaged at least three different fields of view at three different locations on the wafer so that a minimum of 300 particles was characterized per sample.

The chemical composition of the particles was determined using Fourier transform infrared (FTIR) spectrometry

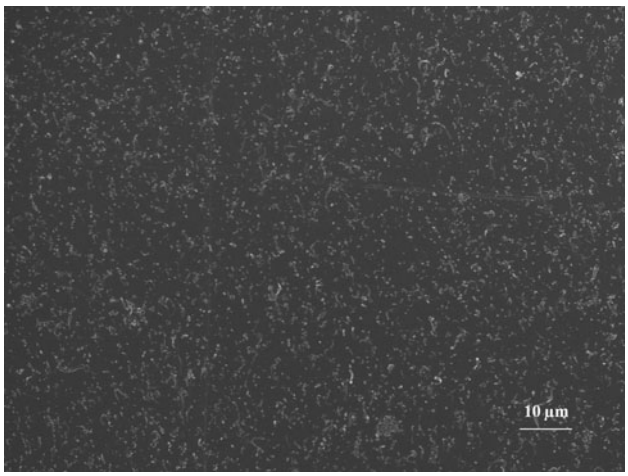


**Fig. 3A** FE-SEM secondary electron image (accelerating voltage, 15 kV; spot size, 1 nm) shows noncrosslinked PE particles recovered with the SWD protocol and displayed on a silicon wafer.

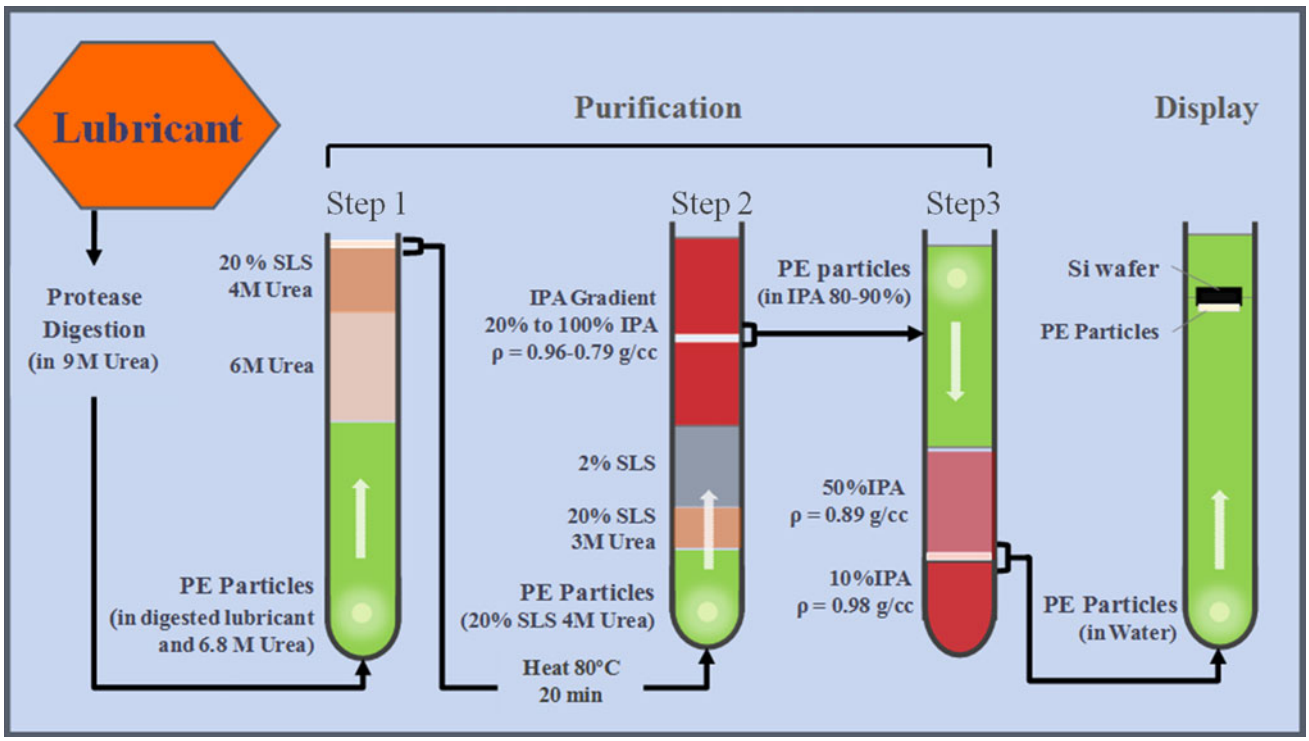


**Fig. 2** A schematic diagram shows the SWD protocol, highlighting the digestion, purification, and display phases.

(Nicolet iS10 FTIR equipped with Centaurus microscope; Thermo Fisher Scientific Inc, Waltham, MA, USA). We verified the debris as PE by the presence on the FTIR spectrum of a carbonyl peak located between 1689 and 1756 $cm^{-1}$.

Finally, particles were characterized morphologically via digital image processing (MetaMorph™ 6.3r7; Molecular Devices Corp, Sunnyvale, CA, USA) and extraction of particle characteristics with dedicated algorithms (Appendix 1).

Commercially available particles differ in range of size and in morphology from particles found in vivo or in joint simulator studies. Therefore, we produced a control as follows. Particles from a single lubricant were isolated and characterized by SWD, eluted from three analyzed wafers using 0.5 mL glacial acetic acid to dissolve the mussel glue, and pooled. This was repeated for each station and each PE type. Each population of particles was then neutralized with 5 N NaOH, lyophilized, mixed with naïve serum, and sonicated four times before the particles were reisolated using the complete SWD and NaOH protocols (Fig. 1). To compare filtration to wafer display, the same volume of samples was used for the filter and for the wafer, and the particle suspension was passed through an area of filter equivalent to the cross-sectional area of the silicon wafer. Reisolated particles were compared with those on the source wafers from the original SWD protocol to determine morphologic characteristics, size distribution, and recovery rate for each method.

We performed statistical analysis (SPSS® Version 14; IBM Corp, Somers, NY, USA) to assess how uniformly the particles were distributed on the wafer and to establish the minimum number of images necessary to accurately determine the distributions. For this, routine descriptive measures, including skewness and kurtosis, were calculated. As expected, the distributions were not normal for any of the parameters. The distributions then were graphed using frequency counts and distribution bar plots. The particle distributions were compared between two samples using the Kolmogorov-Smirnov Z test. P-P plots were constructed for each parameter and were used to compare the distributions among different images within a sample and among different samples.

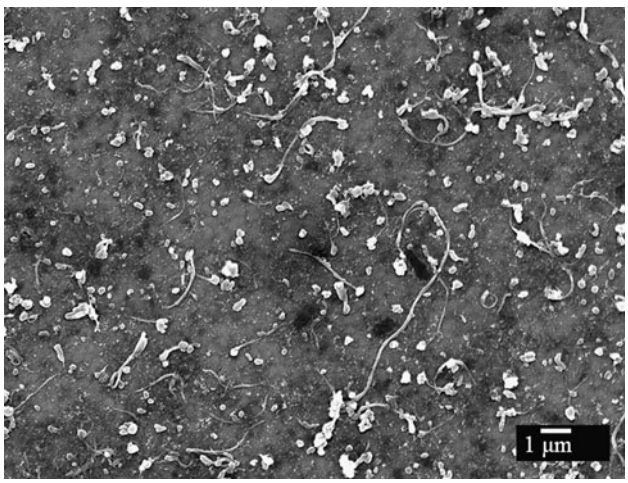


**Fig. 4** A FE-SEM secondary electron image (accelerating voltage, 15 kV; spot size, 1 nm) shows noncrosslinked PE particles recovered with the NaOH protocol and displayed on a PC filter membrane (0.01 µm).

## Results

Compared to the particles isolated on the PC filter using the NaOH protocol (Fig. 4), the particles isolated with the SWD exhibited better separation and minimal clumping and few, if any, contaminants (Fig. 5). When comparing

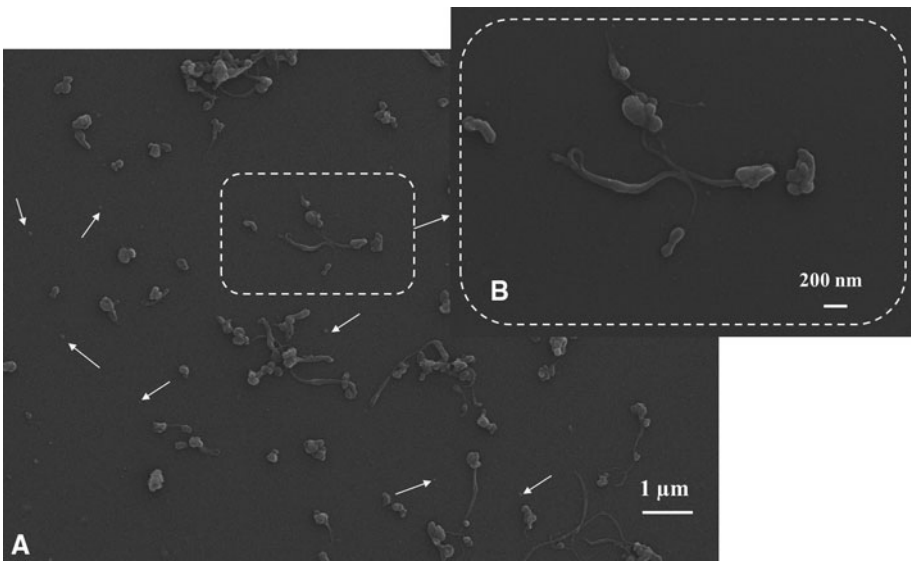


**Fig. 5A–B** FE-SEM images show particles isolated by the SWD protocol and displayed on a silicon wafer. (**A**) This image was selected from among those showing the highest presence of agglomerates, likely formed during the wear process. (**B**) In the inset, fibril-like particles appear to be a complex network of particles of different shape and size "fused" together. These structures formed during the wear process suggest a specific wear mechanism that produced irresolvable agglomerates, confirming what has already been suggested by others. The high power and sensitivity of the SWD protocol allow separation and characterization of particles as small as 20 to 80 nm (arrows).

the percentage of clumping, the difference between the two methods was considerable. For crosslinked PEs, the mean (± SD) percentage of clumping with the NaOH method was 49% ± 19%, whereas for the SWD protocol, it was 6% ± 4%.

The SWD protocol showed, for each of the three PEs and for either of the isolation protocols, the majority of the particles were round and oval shaped, but the noncrosslinked PE contained the highest percentage of rod-, irregular-, and fibril-shaped particles (Table 2). Comparison of the size of the particles between the NaOH and the SWD protocols (Table 3) showed average values that were greater ($p = 0.02$) for the NaOH protocol, indicating possible agglomeration of the smallest particles. Furthermore, unlike the NaOH protocol, the SWD protocol was able to detect differences ($p = 0.04$) in the average maximum Feret's diameters ($d_{max}$) between the two crosslinked PEs as low as 0.1 μm. Even at the highest resolution, the particles were easily distinguishable from the wafer background, which facilitated morphologic analysis, even of the nanometer-sized particles (Fig. 5). The clarity and contrast of the particles on the wafer provided a correspondingly high level of detail in the size distributions (Fig. 6A). By plotting the same data as a continuous profile, differences among sample types were more readily apparent (Fig. 6B). In comparison to noncrosslinked PE, the crosslinked PEs had higher percentages ($p = 0.045$) of particles in the 20- to 60-nm range and in the 300- to 500-nm range but a lower percentage ($p = 0.04$) in the 60- to 300-nm range. Importantly, the local peaks in the distributions occurred at identical locations for the two types of crosslinked PEs and were distinct from the peaks

**Table 2.** Mean particle sizes ($d_{max}$)

| Type of polyethylene | $d_{max}$ (μm) | |
|---|---|---|
| | NaOH protocol | SWD protocol |
| Noncrosslinked | 0.9 ± 0.6 | 0.5 ± 0.2 |
| 5-Mrad crosslinked | 0.5 ± 0.3 | 0.3 ± 0.1 |
| 7.5-Mrad crosslinked | 0.5 ± 0.3 | 0.2 ± 0.09 |

Values are expressed as mean ± SD; $d_{max}$ = maximum Feret's diameter; NaOH = sodium hydroxide; SWD = silicon wafer display.

**Table 3.** Shape distribution among the three polyethylene types

| Shape | Distribution (%) | | |
|---|---|---|---|
| | Noncrosslinked polyethylene | 5-Mrad crosslinked polyethylene | 7.5-Mrad crosslinked polyethylene |
| Round | 29.0 ± 3.2 | 42.8 ± 6.4 | 48 ± 7 |
| Oval | 26.2 ± 1.6 | 34 ± 3.4 | 28.9 ± 3.6 |
| Rod | 20.0 ± 2.8 | 10 ± 2.8 | 8 ± 2.5 |
| Irregular | 21.7 ± 5.4 | 12.7 ± 2.4 | 15 ± 4 |
| Fibril | 3.1 ± 2.0 | 0.5 ± 0.2 | 0.1 ± 0.06 |

Values are expressed as mean ± SD.

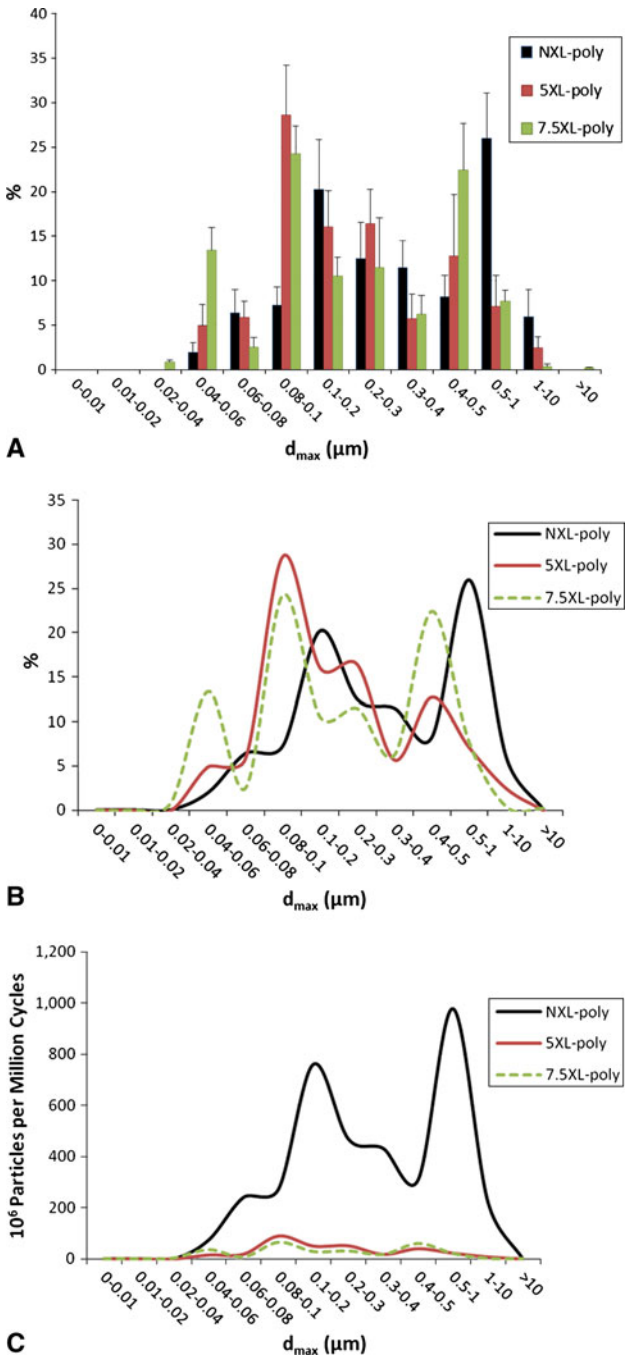


**Fig. 6A–C** Graphs show the size distribution according to (**A**) maximum Feret's diameter ($d_{max}$), (**B**) as percentage of total particles, and (**C**) as relative number of particles per million cycles. NXL-poly = noncrosslinked PE; 5XL-poly = 5-Mrad crosslinked PE; 7.5XL-poly = 7.5-Mrad crosslinked PE.

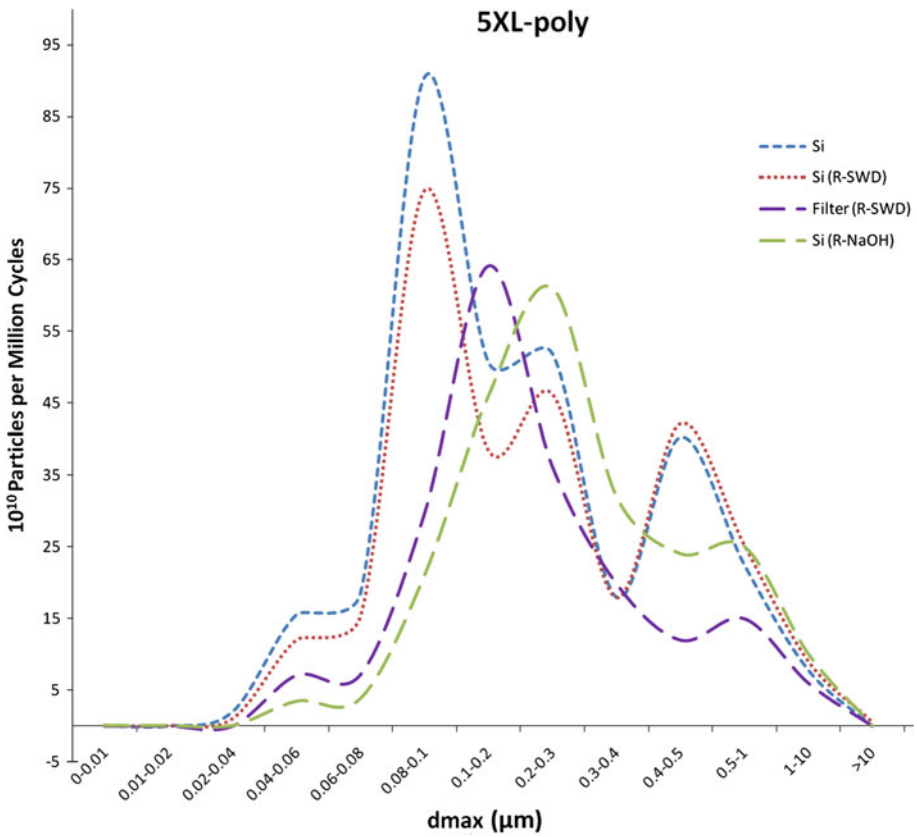


**Fig. 7** A graph illustrates the results of the particle recovery experiments. The size distribution of 5-Mrad crosslinked PE (5XL-poly) particles after isolation by the SWD method is shown (blue line). Particles on these wafers were the source of particles for all other curves: after reisolation from serum by SWD digestion (R-SWD) and display on a silicon wafer (red line); after reisolation from serum by SWD digestion (R-SWD) and display on a filter membrane (green line); and after reisolation from serum by NaOH digestion (R-NaOH) and display on a silicon wafer (dotted purple line).

for the noncrosslinked PE. This indicated radiation crosslinking induced similar changes in the molecular structure for both doses (ie, 5 and 7.5 Mrads). These subtle differences were not detectable with the previous protocol. In addition to the systematic differences in shape and size distribution, compared to noncrosslinked PE, the number of particles produced per million wear cycles was smaller ($p = 0.04$) for the two crosslinked PEs across the entire size spectrum (Fig. 6C).

The results of the control/recovery rate experiment (Fig. 7) indicated close agreement of the size distributions between the original sample and that recovered after reisolation using the SWD protocol. In contrast, the size distribution was shifted toward the large end of the spectrum with the NaOH filtration protocol, probably due to loss of smaller particles, especially in the 0.06- to 1.0-µm range, combined with artifactual clumping generated during digestion/filtration. Quantitatively, the SWD protocol recovered 82% ± 10% of the particles in the original sample, compared to only 47% ± 15% with the filtration protocol ($p = 0.05$).

## Discussion

In vitro models have shown the osteolytic potential of PE wear debris is affected by volume of particles, as well as their size distribution [17, 21, 22, 36]. With followup exceeding 12 years, the incidence and extent of osteolysis have been markedly lower for hip arthroplasties using crosslinked PEs [5, 27, 28]. This outcome contradicts the predictions by some early studies [11, 18, 25], which indicated the osteolytic potentials with elevated crosslinking could be as high as or higher than for historical PEs. Our results indicated this misprediction was in great part due to inherent limitations of the protocols used to isolate and characterize the PE wear particles generated in laboratory wear simulations. We therefore described a novel protocol to meet the demands of analyzing newer crosslinked PE particles and our efforts to validate this protocol.

We note the following limitations to our new approach and the specific experiments. First, the protocol although highly sensitive, is very time consuming, especially the part relative to the morphologic characterization of the particles. Ideally, a faster method for characterizing the particles, if available, should be selected. Second, in the control experiment, we recovered particles deposited on silicon wafers by extracting them with acetic acid. This might have led to loss of particles and contributed to the recovery we reported. Third, while the SWD protocol was designed to minimize clumping, thereby providing highly accurate data on the size and morphology of the individual wear particles, it is possible that some clumping of the particles occurs naturally during wear of a prosthesis, but

also is eliminated by the SWD protocol along with the artifactual clumping. Extensive additional research would be required to determine whether natural clumping occurs and, if so, to identify the mechanism causing it, and, eventually, to develop a digestion protocol that would preserve natural clumping while minimizing artifactual clumping.

In previous studies [3, 38], the efficacy of digesting proteins using proteinase K was compared to other enzymes, as well as acids and bases. However, the conditions used for proteinase K digestion were not optimal as they lacked protein denaturants and proteinase K stabilization. In addition, the use of detergent to solubilize and denature proteins during or after proteolysis yielded partial trapping of PE nanoparticules in detergent micelles, preventing them from reaching their respective equilibrium densities. Complete digestion was obtained with high concentrations of urea to denature proteins and calcium to stabilize proteinase K. Postdigestion calcium chelation, disulfide reduction, and continued denaturation by urea enabled particles to be readily floated away from the small peptides of the digest before introduction of detergent. Thus, detergent excess removed minor contaminants from particles without forming peptide-particle-detergent micelles.

The SWD provided an optimum, featureless background for morphometric analysis and no opportunity for nanometer-sized particle loss or aggregation as occurred with filters (Fig. 4). Sampling errors were minimized, leading to a more accurate determination of particle count and size distribution. SWD was also extremely sensitive to contaminants that might pass through filter pores, the absence of which demonstrated the purity of the particles.

The larger sizes of the particles recovered with the NaOH protocol than with the SWD protocol (Fig. 7) was likely due to partial loss of smaller particles, that is, through filter pores, as well as clumping of smaller particles, which could account for apparently higher percentages of irregular-shaped particles recovered with the NaOH protocol. Excessive clumping can be caused by contaminants. For example, in the NaOH protocol, particles moved away from the gradient rather than through it, concentrating them but not completely separating them from partially digested proteins. These artifacts were avoided by the SWD process, which passed particles through cleaning reagents before display.

Three different experiments demonstrated the advantages of the present method and the relative inadequacy of the previous NaOH protocol. First, from the same sample of wear lubricant, SWD provided smaller average particle sizes than the NaOH protocol. Second, using particles already purified and characterized by the SWD protocol, reisolation from serum with SWD and display by filtration (Fig. 7, green line) led to clumping with increased apparent particle size, fewer size classes, and lower recovery when compared to the original particles (Fig. 7, blue line) and those repurified by the entire SWD protocol (Fig. 7, red line). Third, using SWD-derived particles, repurification from serum through the NaOH protocol followed by SWD rather than filter display led to both increased apparent particle size and lower recovery (Fig. 7, purple line). In each case, the differences represent artifacts induced by the operation of the NaOH protocol or the use of filtration, rather than intrinsic differences in the characteristics of the original particle population.

Endo et al. [11] concluded the functional biologic activity (FBA) of a moderately crosslinked PE (4 Mrads) was not lower than that of a noncrosslinked PE. As noted, this contradicts subsequent clinical experience [5, 28]. In addition to the limitations of the filtration-based protocol employed by Endo et al. [11], they assumed biologic activity indices obtained from in vitro tests of particles from noncrosslinked PE particles also applied to crosslinked PE particles within the same size band. However, SWD images demonstrated differences in the morphology of noncrosslinked and crosslinked PE particles that could affect their relative FBA.

The SWD protocol has demonstrated reproducible differences in the size profile of conventional and highly crosslinked PEs. These differences were not restricted to small and large particles but were also marked in the midrange. The fact that none of the four size maxima exhibited by the highly crosslinked PEs were shared with conventional PE suggests there are structural differences in the crosslinked PE molecular network driving wear to produce different particles. Crosslinked PE particles may thus differ in their surface properties resulting in decreased aggregation or capacity for cellular activation. While both results would predict a decrease in osteolysis/inflammation in combination with the overall decrease in volume of crosslinked PE particle, careful experimental validation in vitro and in vivo is required to identify the responding cells and the nature of their cytokine response.

In conclusion, the SWD protocol provides a powerful new tool for more complete recovery of wear particles, accurate characterization of their morphology, and production of reproducible and representative samples of high-purity particles. It functions equally well with both crosslinked and conventional PE. Because it does not expose particles to acid or base, the SWD protocol can be used in combination with a similar protocol to simultaneously isolate both metal and PE wear debris, preserving their chemical composition and shape.

**Acknowledgments** The authors acknowledge Patricia Campbell, PhD, for her pioneering research on the isolation and characterization of PE wear debris, and Zhen Lu, PhD, and Fu-Wen Shen, PhD, for

their valuable insight into the wear mechanisms and material properties of UHMWPE.

## References


1. Affatato S, Bersaglia G, Emiliani D, Foltran I, Taddei P, Reggiani M, Ferrieri P, Toni A. The performance of gamma- and EtO-sterilised UHMWPE acetabular cups tested under severe simulator conditions. Part 2. Wear particle characteristics with isolation protocols. *Biomaterials.* 2003;24:4045–4055.
2. Bajorath J, Hinrichs W, Saenger W. The enzymatic activity of proteinase K is controlled by calcium. *Eur J Biochem.* 1988;176: 441–447.
3. Baxter RM, Steinbeck MJ, Tipper JL, Parvizi J, Marcolongo M, Kurtz SM. Comparison of periprosthetic tissue digestion methods for ultra-high molecular weight polyethylene wear debris extraction. *J Biomed Mater Res B Appl Biomater.* 2009;91:409–418.
4. Besong AA, Tipper JL, Ingham E, Stone MH, Wroblewski BM, Fisher J. Quantitative comparison of wear debris from UHMWPE that has and has not been sterilised by gamma irradiation. *J Bone Joint Surg Br.* 1998;80:340–344.
5. Bitsch RG, Loidolt T, Heisel C, Ball S, Schmalzried TP. Reduction of osteolysis with use of Marathon cross-linked polyethylene: a concise follow-up, at a minimum of five years, of a previous report. *J Bone Joint Surg Am.* 2008;90:1487–1491.
6. Campbell P, Doorn P, Dorey F, Amstutz HC. Wear and morphology of ultra-high molecular weight polyethylene wear particles from total hip replacements. *Proc Inst Mech Eng H.* 1996;210:167–174.
7. Campbell P, Kossovsky N, Schmalzried TP. Particles in loose hips. *J Bone Joint Surg Br.* 1993;75:161–162.
8. Campbell P, Ma S, Yeom B, McKellop H, Schmalzried TP, Amstutz HC. Isolation of predominantly submicron-sized UHMWPE wear particles from periprosthetic tissues. *J Biomed Mater Res.* 1995;29:127–131.
9. D'Lima DD, Hermida JC, Chen PC, Colwell CW. Polyethylene cross-linking by two different methods reduces acetabular liner wear in a hip joint wear simulator. *J Orthop Res.* 2003;21: 761–766.
10. Dorr LD, Wan Z, Shahrdar C, Sirianni L, Boutary M, Yun A. Clinical performance of a Durasul highly cross-linked polyethylene acetabular liner for total hip arthroplasty at five years. *J Bone Joint Surg Am.* 2005;87:1816–1821.
11. Endo M, Tipper JL, Barton DC, Stone MH, Ingham E, Fisher J. Comparison of wear, wear debris and functional biological activity of moderately crosslinked and non-crosslinked polyethylenes in hip prostheses. *Proc Inst Mech Eng H.* 2002;216:111–122.
12. Endo MM, Barbour PS, Barton DC, Fisher J, Tipper JL, Ingham E, Stone MH. Comparative wear and wear debris under three different counterface conditions of crosslinked and non-crosslinked ultra high molecular weight polyethylene. *Biomed Mater Eng.* 2001;11:23–35.
13. Engh CA Jr, Stepniewski AS, Ginn SD, Beykirch SE, Sychterz-Terefenko CJ, Hopper RH Jr, Engh CA. A randomized prospective evaluation of outcomes after total hip arthroplasty using cross-linked Marathon and non-cross-linked Enduron polyethylene liners. *J Arthroplasty.* 2006;21:17–25.
14. Fang HW, Hsu SM, Sengers JV. Surface texture design to generate specific sizes and shapes of UHMWPE wear particles. *J Mater Sci Eng Technol.* 2003;34:976–988.
15. Fang HW, Hsu SM, Sengers JV. *Ultra-High Molecular Weight Polyethylene Wear Particle Effects on Bioactivity*. NIST SP-1002. Gaithersburg, MD: National Institute of Standards and Technology; 2003.
16. Firkins PJ, Tipper JL, Ingham E, Stone MH, Farrar R, Fisher J. A novel low wearing differential hardness, ceramic-on-metal hip joint prosthesis. *J Biomech.* 2001;34:1291–1298.
17. Fisher J, Bell J, Barbour PS, Tipper JL, Matthews JB, Besong AA, Stone MH, Ingham E. A novel method for the prediction of functional biological activity of polyethylene wear debris. *Proc Inst Mech Eng H.* 2001;215:127–132.
18. Fisher J, McEwen HM, Tipper JL, Galvin AL, Ingram J, Kamali A, Stone MH, Ingham E. Wear, debris, and biologic activity of cross-linked polyethylene in the knee: benefits and potential concerns. *Clin Orthop Relat Res.* 2004;428:114–119.
19. Geerdink C, Grimm B, Vencken W, Heyligers I, Tonino A. Cross-linked compared with historical polyethylene in THA: an 8-year clinical study. *Clin Orthop Relat Res.* 2009;467:979–984.
20. Geerdink CH, Grimm B, Ramakrishnan R, Rondhuis J, Verburg AJ, Tonino AJ. Crosslinked polyethylene compared to conventional polyethylene in total hip replacement: pre-clinical evaluation, in-vitro testing and prospective clinical follow-up study. *Acta Orthop.* 2006;77:719–725.
21. Green TR, Fisher J, Matthews JB, Stone MH, Ingham E. Effect of size and dose on bone resorption activity of macrophages by in vitro clinically relevant ultra-high molecular weight polyethylene particles. *J Biomed Mater Res.* 2000;53:490–497.
22. Green TR, Fisher J, Stone M, Wroblewski BM, Ingham E. Polyethylene particles of a "critical size" are necessary for the induction of cytokines by macrophages in vitro. *Biomaterials.* 1998;19:2297–2302.
23. Hilz H, Wiegers U, Adamietz P. Stimulation of proteinase K action by denaturing agents: application to the isolation of nucleic acids and the degradation of "masked" proteins. *Eur J Biochem.* 1975;56:103–108.
24. Huang CH, Ho FY, Ma HM, Yang CT, Liau JJ, Kao HC, Young TH, Cheng CK. Particle size and morphology of UHMWPE wear debris in failed total knee arthroplasties—a comparison between mobile bearing and fixed bearing knees. *J Orthop Res.* 2002;20: 1038–1041.
25. Illgen RL 2nd, Bauer LM, Hotujec BT, Kolpin SE, Bakhtiar A, Forsythe TM. Highly crosslinked vs conventional polyethylene particles: relative in vivo inflammatory response. *J Arthroplasty.* 2009;24:117–124.
26. Ingram J, Matthews JB, Tipper J, Stone M, Fisher J, Ingham E. Comparison of the biological activity of grade GUR 1120 and GUR 415HP UHMWPE wear debris. *Biomed Mater Eng.* 2002; 12:177–188.
27. Jacobs CA, Christensen CP, Greenwald AS, McKellop H. Clinical performance of highly cross-linked polyethylenes in total hip arthroplasty. *J Bone Joint Surg Am.* 2007;89:2779–2786.
28. Leung SB, Egawa H, Stepniewski A, Beykirch S, Engh CA Jr, Engh CA Sr. Incidence and volume of pelvic osteolysis at early follow-up with highly cross-linked and noncross-linked polyethylene. *J Arthroplasty.* 2007;22:134–139.
29. Liao YS, Benya PD, McKellop HA. Effect of protein lubrication on the wear properties of materials for prosthetic joints. *J Biomed Mater Res.* 1999;48:465–473.
30. Looney RJ, Schwarz EM, Boyd A, O'Keefe RJ. Periprosthetic osteolysis: an immunologist's update. *Curr Opin Rheumatol.* 2006;18:80–87.
31. Mabrey JD, Afsar-Keshmiri A, Engh GA, Sychterz CJ, Wirth MA, Rockwood CA, Agrawal CM. Standardized analysis of UHMWPE wear particles from failed total joint arthroplasties. *J Biomed Mater Res.* 2002;63:475–483.
32. Manning DW, Chiang PP, Martell JM, Galante JO, Harris WH. In vivo comparative wear study of traditional and highly cross-linked polyethylene in total hip arthroplasty. *J Arthroplasty.* 2005;20:880–886.

33. Matthews JB, Besong AA, Green TR, Stone MH, Wroblewski BM, Fisher J, Ingham E. Evaluation of the response of primary human peripheral blood mononuclear phagocytes to challenge with in vitro generated clinically relevant UHMWPE particles of known size and dose. *J Biomed Mater Res.* 2000;52:296–307.
34. McKellop H, Clarke I, Markolf K, Amstutz H. Friction and wear properties of polymer, metal, and ceramic prosthetic joint materials evaluated on a multichannel screening device. *J Biomed Mater Res.* 1981;15:619–653.
35. McKellop HA, Campbell P, Park SH, Schmalzried TP, Grigoris P, Amstutz HC, Sarmiento A. The origin of submicron polyethylene wear debris in total hip arthroplasty. *Clin Orthop Relat Res.* 1995;311:3–20.
36. Mitchell W, Bridget Matthews J, Stone MH, Fisher J, Ingham E. Comparison of the response of human peripheral blood mononuclear cells to challenge with particles of three bone cements in vitro. *Biomaterials.* 2003;24:737–748.
37. Muratoglu OK, Bragdon CR, O'Connor DO, Jasty M, Harris WH. A novel method of cross-linking ultra-high-molecular-weight polyethylene to improve wear, reduce oxidation, and retain mechanical properties. Recipient of the 1999 HAP Paul Award. *J Arthroplasty.* 2001;16:149–160.
38. Niedzwiecki S, Klapperich C, Short J, Jani S, Ries M, Pruitt L. Comparison of three joint simulator wear debris isolation techniques: acid digestion, base digestion, and enzyme cleavage. *J Biomed Mater Res.* 2001;56:245–249.
39. Rajadhyaksha AD, Brotea C, Cheung Y, Kuhn C, Ramakrishnan R, Zelicof SB. Five-year comparative study of highly cross-linked (Crossfire) and traditional polyethylene. *J Arthroplasty.* 2009;24:161–167.
40. Richards L, Brown C, Stone MH, Fisher J, Ingham E, Tipper JL. Identification of nanometre-sized ultra-high molecular weight polyethylene wear particles in samples retrieved in vivo. *J Bone Joint Surg Br.* 2008;90:1106–1113.
41. Ries MD, Scott ML, Jani S. Relationship between gravimetric wear and particle generation in hip simulators: conventional compared with cross-linked polyethylene. *J Bone Joint Surg Am.* 2001;83(Suppl 2 Pt 2): S116–S122.
42. Saikko V, Calonius O, Keranen J. Wear of conventional and cross-linked ultra-high-molecular-weight polyethylene acetabular cups against polished and roughened CoCr femoral heads in a biaxial hip simulator. *J Biomed Mater Res.* 2002;63:848–853.
43. Schmalzried TP, Campbell P, Schmitt AK, Brown IC, Amstutz HC. Shapes and dimensional characteristics of polyethylene wear particles generated in vivo by total knee replacements compared to total hip replacements. *J Biomed Mater Res.* 1997;38:203–210.
44. Shanbhag AS, Jacobs JJ, Black J, Galante JO, Glant TT. Macrophage/particle interactions: effect of size, composition and surface area. *J Biomed Mater Res.* 1994;28:81–90.
45. Shanbhag AS, Jacobs JJ, Black J, Galante JO, Glant TT. Human monocyte response to particulate biomaterials generated in vivo and in vitro. *J Orthop Res.* 1995;13:792–801.
46. Shanbhag AS, Jacobs JJ, Glant TT, Gilbert JL, Black J, Galante JO. Composition and morphology of wear debris in failed uncemented total hip replacement. *J Bone Joint Surg Br.* 1994;76:60–67.
47. Tipper JL, Galvin AL, Williams S, McEwen HM, Stone MH, Ingham E, Fisher J. Isolation and characterization of UHMWPE wear particles down to ten nanometers in size from in vitro hip and knee joint simulators. *J Biomed Mater Res A.* 2006;78: 473–480.
48. Wang A, Essner A, Stark C, Dumbleton JH. Comparison of the size and morphology of UHMWPE wear debris produced by a hip joint simulator under serum and water lubricated conditions. *Biomaterials.* 1996;17:865–871.
49. Yang SY, Ren W, Park Y, Sieving A, Hsu S, Nasser S, Wooley PH. Diverse cellular and apoptotic responses to variant shapes of UHMWPE particles in a murine model of inflammation. *Biomaterials.* 2002;23:3535–3543.